

LeetDecoding: A PyTorch Library for Exponentially Decaying Causal Linear Attention with CUDA Implementations

Jiaping Wang^{†,‡,*} Simiao Zhang^{†,‡,*} Qiao-Chu He[§] Yifan Chen[†]

[†] Computational Machine Intelligence Laboratory, Hong Kong Baptist University

[‡] Software Engineering Institute, East China Normal University

[§] School of Business, Southern University of Science and Technology

Abstract

The machine learning and data science community has made significant while dispersive progress in accelerating transformer-based large language models (LLMs), and one promising approach is to replace the original causal attention in a generative pre-trained transformer (GPT) with *exponentially decaying causal linear attention*. In this paper, we present LeetDecoding, which is the first Python package that provides a large set of computation routines for this fundamental operator. The launch of LeetDecoding was motivated by the current lack of ❶ clear understanding of the complexity regarding this operator, ❷ a comprehensive collection of existing computation methods (usually spread in seemingly unrelated fields), and ❸ CUDA implementations for fast inference on GPU. LeetDecoding’s design is easy to integrate with existing linear-attention LLMs, and allows for researchers to benchmark and evaluate new computation methods for exponentially decaying causal linear attention. The usage of LeetDecoding does not require any knowledge of GPU programming and the underlying complexity analysis, intentionally making LeetDecoding accessible to LLM practitioners. The source code of LeetDecoding is provided at [this GitHub repository](#), and users can simply install LeetDecoding by the command `pip install leet-decoding`.

1 Introduction

The transformer (Vaswani et al., 2017) architecture, especially since the inception of ChatGPT (OpenAI, 2022), has revolutionized the business application of AI techniques (Caiado & Hahsler, 2023; Li et al., 2024; Brugiare & Turinici, 2024; Yang et al., 2024) particularly through the development of large language models (LLMs). Its core component, the softmax attention, is adept at modeling local and long-range dependencies (Lu et al., 2019; Tian et al., 2022; Wu et al., 2023) and supports parallelized training, but suffers from quadratic complexity in sequence length (Yang et al., 2022). To address the efficiency issue, numerous efforts have been made to accelerate the transformers; notably, the startup company Groq, focusing on improving inference efficiency, had raised a \$640M Series D round at a valuation of \$2.8 billion in 2024 (Groq, 2024).

Linear attention has emerged as a promising alternative, especially for encoder transformers equipped with *bidirectional attention*, by replacing the exponential similarity function in attention with a simple dot product over key/query token vectors (c.f. the introduction in Section 2.2). For

* Equal contribution.

example, Performer (Choromanski et al., 2020) and random feature attention (Peng et al., 2021) decompose the attention weight matrix into a product of two rectangular matrices, respectively consisting of learned linear features or random features (Rahimi & Recht, 2007) of the keys and queries. Skyformer (Chen et al., 2021) employed the Nyström method for efficient computation, while LARA (Zheng et al., 2022) merged randomized attention with random feature attention to effectively reconstruct the attention weight matrix. Moreover, Linformer (Wang et al., 2020) applied Johnson–Lindenstrauss (JL) transforms (Johnson & Lindenstrauss, 1984; Dzahini & Wild, 2024) to attain fast computation; Skeinformer (Chen et al., 2022) generalized the JL transforms to randomized sketching and approximated bidirectional attention with sampling techniques in approximately linear time to improve inference speed. Transformer-VQ (Lingle, 2024) performed “clustering” on the sequence of Key vectors in attention using vector quantization, approximating the original vectors with the centroid of their respective classes.

However, despite the linear scaling in memory / computational requirements and the empirical successes seen in encoder transformers, few linear-attention attempts are made to match the performance of *decoder transformers* (i.e., GPT-like transformers), which are exemplified by ChatGPT and thus the current mainstream paradigm for large language models. Specifically, a decoder block in a transformer will adopt **causal attention** (i.e., unidirectional attention, c.f. Section 2.1), and a vanilla application of linear attention techniques to causal attention (namely **causal linear attention**) will still lead to an $\mathcal{O}(N^2)$ complexity, as shown in Equation (4). This plausible obstacle does hinder the exploration of adapting preceding linear attention methods to causal attention mechanisms; while it turns out the intrinsic complexity for causal linear attention is $\mathcal{O}(N)$ as well, most LLM practitioners are unaware of the analysis result.

Until recently, the *exponential decay of attention scores* has been found useful to bridge the performance gap between causal attention and **causal linear attention**, which is now the de facto configuration taken by various *linear transformers* (linear attention transformers trained from scratch). For example, RWKV (Peng et al., 2023), RetNet (Sun et al., 2023), and TransNormerLLM (Qin et al., 2023) combine causal masking and exponential decay along relative distance into a single matrix. This approach alleviates attention dilution issues while maintaining computational efficiency. Notably, the linear-attention-based LLM, TransNormerLLM, with the design of exponential decay, has been reported to outperform conventional softmax-attention-based models in both accuracy and efficiency (Qin et al., 2023); RWKV, instead of the more prominent model GPT-4, has even been incorporated into the Windows 11 system (Rwkv, 2024) due to its superior efficiency.

In spite of the fast development of linear transformers, existing computation methods are spread in various fields/methods (summarized in Table 1) and are not yet realized by the community of machine learning and data science that they are appropriate to causal linear attention, let alone available via a comprehensive, easy-to-use library. Whereas there are recent studies focusing on optimizing regular linear attention on modern GPUs and give I/O-aware algorithms implementations (Yang et al., 2023), they only implement a specific calculation and does not consider and analyze scenarios under different batch sizes such as in Section 5. Moreover, the code of Yang et al. (2023) is highly coupled and is not well compatible with other large models. There is a strong need for a fast, user-friendly library to efficiently run transformers with exponentially decaying causal linear attention.

1.1 Our contributions

In this work, we thoroughly investigate existing linear-complexity computation algorithms from various fields (not originally for causal linear attention), expanding and adapting these algorithms

Table 1: Overview of the computation methods for causal linear attention.

Computation Method	Source Field	Time Complexity
vanilla (Equation (4))	-	$\mathcal{O}(N^2)$
causal-dot-product (Vyas et al., 2020)	linear attention	$\mathcal{O}(N)$
block-based (Lingle, 2024)	linear transformer	$\mathcal{O}(N)$
recursion (Han et al., 2023)	attention approximation	$\mathcal{O}(N \log N)$
lightningAttention-2 (Qin et al., 2024)	linear transformer	$\mathcal{O}(N)$
FleetAttention (Section 3.1)	this paper	$\mathcal{O}(N)$

for standard low-rank attention. To the best of our knowledge, our work is the first study in this area. Additionally, we provide complexity analyses for multiple computation methods, which are usually dismissed by LLM practitioners. In particular, one recursive computation method (Han et al., 2023) indeed has a suboptimal $\mathcal{O}(N \log N)$ complexity (c.f. Section 3.3) and thus the practical efficiency is inferior to other candidate methods, as shown in Section 5.

More importantly, we introduce LeetDecoding, a Python package that adapts and implements all the preceding computation methods for exponentially decaying causal linear attention, along with a newly proposed algorithm FleetAttention. Furthermore, the package is built on PyTorch with CUDA optimizations to leverage the parallel processing capabilities of modern GPUs. We demonstrate that LeetDecoding is easy to use for individual decoder modules and can be seamlessly incorporated into large language models. These two features are especially useful to LLM practitioners as, in deploying LLMs, intensive performance evaluations are a must to empirically decide the optimal implementations under different scenarios. (See the results in Section 5. No computation method can dominate others along all the settings.)

1.2 Paper organization

In the remainder of this paper, Section 2 introduces necessary notations and preliminaries of exponentially decaying causal linear attention. In Section 3, we introduce the algorithms involved in the package and the CUDA implementation for fast inference on GPU. In Section 4, we demonstrate the usage of the package LeetDecoding, which supports both benchmarking computation methods in individual causal linear attention modules and integrating with existing large linear transformers. Empirical results are provided in Section 5 for both of the settings above. We leave a concluding remark in Section 6.

2 Notations and Preliminaries

For the reader’s convenience, we introduce the standard attention mechanism as a preliminary in Section 2.1. Exponentially decaying causal linear attention, the core of this library, is then introduced in Section 2.2.

2.1 Standard attention mechanisms

The dot-product attention (Vaswani et al., 2017) processes three input matrices $\mathbf{Q}, \mathbf{K}, \mathbf{V} \in \mathbb{R}^{N \times d}$, wherein N is the number of tokens in the input sequence and d denotes the head dimension. On one hand, the bidirectional attention, the first-generation attention proposed in the BERT language

model (Devlin et al., 2018), is defined as:

$$\mathbf{D}^{-1}\mathbf{A}\mathbf{V} \tag{1}$$

Here the matrix $\mathbf{A} = \exp(\mathbf{Q}\mathbf{K}^T) \in \mathbb{R}^{N \times N}$ represents the element-wise exponential of $\mathbf{Q}\mathbf{K}^T$ (for simplicity, the normalization factor \sqrt{d} has been omitted). The diagonal matrix $\mathbf{D} = \text{diag}(\mathbf{A}\mathbf{1}_N)$ contains the row sums of \mathbf{A} along its main diagonal, where $\mathbf{1}_N$ is a length- N all-ones vector. In this context, matrix \mathbf{A} is called the *attention matrix* or *attention score matrix*.

On the other hand, causal attention (or unidirectional attention) is used for auto-regressive generative modeling, such as the decoder components of ChatGPT and its successor GPT-4 (OpenAI, 2022). It is defined as:

$$(\mathbf{D}')^{-1}(\mathbf{A} \odot \mathbf{M})\mathbf{V}, \quad \text{where } \mathbf{D}' = \text{diag}((\mathbf{A} \odot \mathbf{M})\mathbf{1}_N), \tag{2}$$

and $\mathbf{M} \in \{0, 1\}^{N \times N}$ is a lower triangular matrix:

$$\mathbf{M}_{i,j} = \delta(i, j) := \begin{cases} 1, & \text{if } i \geq j, \\ 0, & \text{otherwise.} \end{cases}$$

The time complexity for computing both Equation (1) and Equation (2) is $\mathcal{O}(N^2d)$. Their space complexity is $\mathcal{O}(N^2 + Nd)$, which is due to the explicit use of the attention matrix \mathbf{A} .

2.2 (Exponentially decaying) Causal linear attention

Researchers have invented various linear-attention large language models to mitigate the quadratic computational complexity associated with standard attention mechanisms, including TransNormerLLM (Qin et al., 2023), RetNet (Sun et al., 2023), RWKV (Peng et al., 2023), and Mamba (Gu & Dao, 2023). The computation of attention matrix in these linear attention models can all be abstracted into a low-rank form involving matrices $\mathbf{B}, \mathbf{C} \in \mathbb{R}^{N \times d}$ where we formally remove the element-wise exponential function and the row normalization in Equation (1). A universal formula,

$$\mathbf{A} = \mathbf{B}\mathbf{C}^T, \tag{3}$$

can succinctly describe the attention matrix functionality within these models and is used along this paper. For TransNormerLLM and RetNet, for example, $\mathbf{B} = \mathbf{Q}$, $\mathbf{C} = \mathbf{K}$.

With Equation (3) at hand, we can formulate the *exponentially decaying causal linear attention* as follows:

$$(\mathbf{B}\mathbf{C}^T \odot \mathbf{M})\mathbf{V} \tag{4}$$

where the lower triangular matrix \mathbf{M} is now reloaded, with

$$\mathbf{M}_{i,j} = \delta(i, j) := \begin{cases} \gamma^{i-j}, & \text{if } i \geq j, \\ 0, & \text{otherwise.} \end{cases}$$

In the case $\gamma = 1$, Equation (4) will be simply dubbed *causal linear attention*.

In addition to the aforementioned linear attention adopted in a native linear transformer, all *low-rank approximation methods* can be similarly unified in the form of Equation (3). Low-rank approximation methods, when applied to bidirectional attention mechanism, involve the utilization of two matrices $\mathbf{B}, \mathbf{C} \in \mathbb{R}^{N \times r}$ of low rank (here we reload the notations for arbitrarily two matrices \mathbf{B}, \mathbf{C}), to approximate the attention matrix \mathbf{A} through $\hat{\mathbf{A}} = \mathbf{B}\mathbf{C}^T$, where r indicates the rank of $\hat{\mathbf{A}}$

and conceptually differs from the previous (head) dimension d . We illustrate the ubiquity of the approximation framework above through dissecting Transformer-VQ (Lingle, 2024) as an example; in their approximation method, $\mathbf{B} = \mathbf{Q}$ and $\mathbf{C} = VQ(\mathbf{K}, \mathbf{c})$ where \mathbf{c} is a codebook.

In applying those low-rank techniques for either linear attention or attention approximation, however, we formally still need to first obtain Equation (4);

however, due to the application of a mask to $\tilde{\mathbf{A}}$, we cannot directly utilize the low-rankness thereof and reduce the computation complexity by matrix right-multiplication as in bidirectional attention. A naïve implementation of Equation (4) still leads to a time complexity $\mathcal{O}(N^2r + N^2d)$ and memory complexity $\mathcal{O}(N^2 + Nd)$. Shortly in Section 3.1, we will illustrate the intrinsic linear complexity of Equation (4) through introducing a new *computation method*, FleetAttention, which rearrange the computation process of Equation (4) to attain linear complexity.

3 Algorithms and Library Design

The overall goal of our library is to enhance the computational efficiency of the attention component in transformer models. In Section 3.1, we introduce a novel computation method named FleetAttention for calculating causal linear attention and showcase its intrinsic linear complexity. Section 3.2 lists all the collected efficient methods (to the best of our knowledge) for computing linear attention that are implemented in our library. In Section 3.3, we analyze the asymptotic suboptimality of using recursive methods for computing linear attention. Finally, Section 3.4 delves into the specific implementation details of the methods within our library.

3.1 A non-iterative matrix formulation for exponentially decaying causal linear attention

In this section, we introduce a new computation method named FleetAttention for computing exponentially decaying causal linear attention. Our method employs a non-iterative matrix formulation and thus clearly exhibits the intrinsic complexity of exponentially decaying causal linear attention.

Given the input matrices $\mathbf{B}, \mathbf{C}, \mathbf{V}$, our objective is to compute the attention output \mathbf{O} with linear compute complexity. Here, we mainly describe how to compute $\mathbf{O} := (\mathbf{BC}^T \odot \mathbf{M})\mathbf{V}$ in Equation (4). To ease the derivation, we denote $\mathbf{b}_i, \mathbf{c}_i$ respectively as the i -th column of \mathbf{B}, \mathbf{C} , and thus \mathbf{BC}^T amounts to $\sum_i \mathbf{b}_i \mathbf{c}_i^T$. We then have:

$$\mathbf{O} = \sum_{i=1}^r \left((\mathbf{b}_i \mathbf{c}_i^T) \odot \mathbf{M} \right) \mathbf{V} = \sum_{i=1}^r \text{diag}(\mathbf{b}_i) \mathbf{M} \text{diag}(\mathbf{c}_i) \mathbf{V},$$

in which the second equation holds due to the known property of Hadamard product. For a classic causal mask with binary elements in $\{0, 1\}$, we leverage the special structure of the mask matrix \mathbf{M} that it is equivalent to a cumsum (cumulative sum) operator, we finally obtain

$$\mathbf{O} = \sum_{i=1}^r \text{diag}(\mathbf{b}_i) \text{cumsum}(\text{diag}(\mathbf{c}_i) \mathbf{V}), \quad (5)$$

where the cumsum operator is applied to the column vectors of matrix $\text{diag}(\mathbf{c}_i) \mathbf{V}$ in parallel. We note in obtaining each summand the time complexity is $\mathcal{O}(Nd)$, and therefore the total computation complexity will remain $\mathcal{O}(Ndr)$. The algorithm above can be generalized to a popular attention variant with exponentially decaying positional weights (Press et al., 2022; Qin et al., 2022; Peng et al., 2023), and the corresponding derivation is provided in Appendix C.1.

The FleetAttention method has been incorporated into the library, as shown in Section 3.2. As a closing remark, although this method clearly showcases the intrinsic linear complexity of exponentially decaying causal linear attention, fine-grained CUDA programming cannot apply to its practical implementation as most of its calculation process is Hadamard product, rather than conventional matrix multiplication favored by GPU. Although operations along the rank dimension can be performed in parallel, the final process of summing up the results is mutually exclusive and must be carried out serially; detailed analysis is deferred to Appendix D.

3.2 Implemented methods

We unearth the algorithms for causal linear attention from the literature in various fields (we indeed generalize some methods from their original settings to low-rank causal attention), and prepare the PyTorch implementation if originally unavailable. Table 1 has already presented a comprehensive overview of existing computation algorithms. We give a brief introduction to each algorithm in the following list; more detailed description, including how to generalize them from the original setting, are provided in Appendix B.

vanilla. The direct computation of Equation (4) using PyTorch. We implemented the computation with both casual masks that employ binary values in $\{0, 1\}$ and masks with exponentially decaying positional embedding.

causal-dot-product. This algorithm was first introduced by Vyas et al. (2020) as the CausalLinearAttention class in their Fast Transformers library¹ (while this algorithm was not detailed and explained in their paper). This algorithm utilizes the dot product between feature maps (\mathbf{B}, \mathbf{C}) and leverages the triangular structure of the causal masking to compute the attention outputs row by row, achieving linear time complexity. Choromanski et al. (2020) reinvented the computation method causal-dot-product for addressing general low-rank formats, as the algorithm description in their appendix is consistent with the code of causal-dot-product. Full details of this algorithm can be seen in Appendix B.1.

The official CUDA implementation of causal-dot-product by Vyas et al. (2020) solely supports the fp32 type and the classic causal linear attention calculations with masks consisting exclusively of 0s and 1s on GPU. We modified its code to support both fp32 and fp16 types, as well as the causal masks with exponentially decaying positional embedding. Moreover, as there is no native PyTorch implementation provided in either Vyas et al. (2020) or Choromanski et al. (2020), we develop a PyTorch version of causal-dot-product, i.e., causal-dot-product_torch, for the library user’s convenience.

block-based. In the attention approximation method Transformer-VQ (Lingle, 2024), they proposed an algorithm to accelerate causal linear attention computation through a block-by-block approach. The original design is uniquely tailored to the vector-quantized keys and initially applied in a gated activation unit (GAU). We have extended this algorithm to a more general low-rank factorization format as in Equation (4). The extended algorithm is detailed in Appendix B.2 and implemented using PyTorch.

recursion. Han et al. (2023) proposed to compute causal linear attention by dividing the attention matrix into masked and unmasked submatrices (c.f. Appendix B.3); then, they utilized sparse

¹See <https://github.com/idiap/fast-transformers>.

attention to accelerate the computation of the unmasked submatrix, while continuing to recursively divide the masked submatrices. For the PyTorch implementation in `LeetDecoding`, we substantially improve its computational efficiency by running `causal-dot-product` to calculate its base case.

lightningAttention-2. [Qin et al. \(2024\)](#) leveraged the concept of “divide and conquer” by separately handling the intra-block and the inter-block components in causal linear attention calculation. They divide a long input sequence into multiple blocks; inside a block, they simply use `vanilla` to compute the product $(\mathbf{BC}^T \odot \mathbf{M})\mathbf{V}$, while at the inter-block level they follow `causal-dot-product` and apply the similar linear attention kernel trick. More algorithm details can be seen in Section 3.2 of [Qin et al. \(2024\)](#).

Its original code is implemented by OpenAI Triton while does not support the `fp32` type, and even only supports NVIDIA A100 GPU; the causal masks involved are required to have exponentially decaying positional embedding. To generalize their implementation for other scenarios, we modified its source code so that the subroutine can run on GPUs other than NVIDIA A100, allow `fp32` types, and natively support regular causal masks with binary values. In addition, we also implemented this method in PyTorch and named it `lightningAttention-2_torch` for more comprehensive evaluation.

FleetAttention. We recall the method proposed in Section 3.1 adopts a non-iterative matrix formulation to compute causal linear attention; through leveraging the cumulative sum (`cumsum`) operation in Equation (5), the computational complexity is reduced to $\mathcal{O}(N)$.

We used OpenAI Triton to write the core algorithm of `FleetAttention` and supported causal masks with both binary values in $\{0, 1\}$ and exponentially decaying positional embedding. (The details of its GPU programming can be found in Appendix B.4.) Its native PyTorch implementation is provided in `LeetDecoding` as well and named `FleetAttention_torch`.

3.3 Asymptotic suboptimality of recursive computation method

An interesting observation of the lower triangular matrix \mathbf{M} is that the product $(\mathbf{M} \odot \tilde{\mathbf{A}})\mathbf{V}$ can be rewritten in a partitioned manner (for simplicity we omit the dependence on $\tilde{\mathbf{A}}$ in the notations of \mathbf{M}_i ’s):

$$\begin{pmatrix} \mathbf{M}_1 & \mathbf{0} \\ \mathbf{M}_2 & \mathbf{M}_3 \end{pmatrix} \begin{pmatrix} \mathbf{V}_1 \\ \mathbf{V}_2 \end{pmatrix} = \begin{pmatrix} \mathbf{M}_1 \mathbf{V}_1 \\ \mathbf{M}_2 \mathbf{V}_1 + \mathbf{M}_3 \mathbf{V}_2 \end{pmatrix}, \quad (6)$$

where $\mathbf{M}_1, \mathbf{M}_3$ are two smaller lower triangular matrices and \mathbf{M}_2 in the bottom left corner of $\mathbf{M} \odot \tilde{\mathbf{A}}$ is a regular dense matrix. Realizing the observation, [Han et al. \(2023\)](#) mentioned a scheme to efficiently compute their proposed low-rank attention in decoders: we can normally compute the product $\mathbf{M}_2 \mathbf{V}_1$ and then recursively address the two smaller matrices $\mathbf{M}_1 \mathbf{V}_1$ and $\mathbf{M}_3 \mathbf{V}_2$.

The recursive strategy stands distinct from other efficient causal linear attention computation methods. Although the strategy is attractive at first sight, we note it suffers from several deficiencies, ① higher time complexity and ② inefficient hardware implementation.

① As shortly delineated in Lemma 3.1, even equipped with an efficient $\mathcal{O}(N)$ low-rank attention computation method, the recursive approach is characterized by a computational complexity of $\mathcal{O}(N \log N)$, with its proof detailed in Appendix C.2. We note the recursive strategy exhibits a higher complexity than the original $\mathcal{O}(N)$ low-rank attention computation method.

Table 2: The programming language used to implement the methods in the LeetDecoding library. ‘-’ indicates the PyTorch implementation is already sufficient and a CUDA implementation cannot further accelerate the method.

Method name	PyTorch impl.	CUDA impl.	Abbreviation
vanilla	✓	-	Vanilla
block-based	✓	-	Bb
causal-dot-product	✓	Native CUDA	Cdotp
FleetAttention	✓	OpenAI Triton	FA
lightningAttention-2	✓	OpenAI Triton	LA
recursion	✓	-	Recur

Lemma 3.1. *Consider the matrices $\mathbf{B}, \mathbf{C} \in \mathbb{R}^{N \times r}$, $\mathbf{V} \in \mathbb{R}^{N \times d}$, $\tilde{\mathbf{A}} = \mathbf{BC}^T$, and the causal mask matrix \mathbf{M} . The time complexity of using the recursive computation method to compute $(\tilde{\mathbf{A}} \odot \mathbf{M})\mathbf{V}$, even equipped with a linear-complexity algorithm to compute the base case, is $\mathcal{O}(N \log N)$.*

② In addition, GPUs are designed to optimize large-scale, parallel data processing, while recursion involves deeply nested calls and complex control flows, which is inconsistent with the advantages of modern hardware. Combining ① and ②, we conclude the recursive computation method is sub-optimal for decoding extremely long prompts on GPUs.

3.4 Fast inference on GPU and CUDA implementation

Implemented in PyTorch, all the methods in Section 3.2 can naturally run on GPU. For most methods, the native PyTorch implementation is sufficient; however, for `causal-dot-product`, `lightningAttention-2`, and `FleetAttention`, lower-level GPU programming in languages such as native CUDA and OpenAI Triton can improve parallelism and better utilize GPU resources. To more efficiently leverage the computational power of GPUs, we heavily optimize the CUDA implementations of the three methods above, and details can be found in Appendix B.5.

In Section 5.1, we exhibit the efficiency difference between the CUDA implementation and the native PyTorch implementation; the former in most cases is more than twice faster than the counterpart native PyTorch implementation. Table 2 summarizes the implementation status of the methods in LeetDecoding, and remarkably all of them support both fp16 and fp32 types on GPU.

4 How to Use LeetDecoding

We introduce how LeetDecoding is designed to serve various LLM practitioners. At the end of this section, we as well provide a snippet to demonstrate the practical usage of LeetDecoding.

① For application developers adopting linear transformers to achieve supreme inference efficiency, LeetDecoding can be integrated into transformer-based models through its API. For transformer-based models, you can directly replace the original attention computation interface with LeetDecoding for attention calculation. The input format of this library is consistent with the most popular computation libraries like HuggingFace Transformers² or FlashAttention³.

²See <https://github.com/huggingface/transformers>

³See <https://github.com/Dao-AI/flash-attention>

Listing 1: An example of how to use LeetDecoding Library to benchmark your own implementation.

```
1 from efficient_linear_decoding.test_method import benchmark_method
2
3 def attn(q, k, v, gamma):
4     # customize the linear attention computation method here.
5     pass
6
7 # Example usage of the benchmark_method() function:
8 # Note: The values below should be replaced with the most suitable values.
9
10 benchmark_method(method=attn, device='cuda', dtype='float32', batch_size=16,
11                 is_weight_decay=True, gamma=gamma)
```

② For researchers in the community of machine learning and data science, LeetDecoding can serve as a benchmark for profiling the newly proposed linear attention algorithms, as shown in Listing 1. LeetDecoding is intentionally designed for easy extension, and new computation methods can be implemented therein through creating the corresponding method class and subsequently registering the class in LeetDecoding.

To demonstrate the simplicity and the convenience of the coding style in LeetDecoding, we provide another snippet to show how LeetDecoding solves synthetic problems efficiently by a few lines of code. Specifically, Listing 2 gives three examples to illustrate how to use the LeetDecoding library, ranging from the passing of input arguments, to the specification of the mask type and the computation method.

Listing 2: Inference using the causal_linear_decoder requires one line for regular causal attention or two lines with exponentially decaying mask.

```
1 from efficient_linear_decoding import causal_linear_decoder
2
3 batch_size, heads, seqlen, rank = 1, 32, 4096, 128
4 dim = 256
5 B = torch.randn((batch_size, heads, seqlen, rank), device='cuda')
6 C = torch.randn((batch_size, heads, seqlen, rank), device='cuda')
7 V = torch.randn((batch_size, heads, seqlen, dim), device='cuda')
8 gamma = torch.full((heads, 1), 0.9, device='cuda')
9
10 # If the user intends to apply a 0-1 causal mask.
11 output = causal_linear_decoder(B, C, V)
12
13 # If the user intends to apply an exponentially decaying mask.
14 output = causal_linear_decoder(B, C, V, is_mask_weight=True, gamma=gamma)
15
16 # If the user intends to apply a specified method in the library.
17 output = causal_linear_decoder(B, C, V, attn_method='block-based')
```

5 Empirical Results

We report the empirical results in this section. In Section 5.1, we evaluate the computational performance of implementations in our library when handling *extremely long prompts*. Then in Section 5.2, we evaluate the aforementioned computation methods under different settings on pretrained linear transformers. Moreover, along this section we adopt the abbreviations in Table 2 to simplify the presentation.

Table 3: Measured latency (s) of single-layer attention with batch size 1 without exponentially decaying causal mask.

Method \ SeqLen	128	512	2,048	8,192
Vanilla	9.56e-5 \pm 3.7e-7	3.92e-4 \pm 2.7e-7	5.91e-3 \pm 7.7e-6	9.4e-2 \pm 1e-4
Bb	1.06e-3 \pm 4.5e-5	4.8e-3 \pm 5.1e-4	1.84e-2 \pm 4.7e-4	7.08e-2 \pm 1.1e-3
Cdotp	2.36e-4 \pm 2.2e-7	9.32e-4 \pm 2.7e-6	3.7e-3 \pm 6.8e-6	1.6e-2 \pm 2.4e-5
Cdotp_torch	1.43e-2 \pm 3.6e-5	5.61e-2 \pm 3.5e-5	2.25e-1 \pm 8.6e-5	1.21 \pm 4.1e-4
FA	1.26e-3 \pm 8.2e-6	5.46e-3 \pm 1.9e-5	2.72e-2 \pm 1.2e-5	1.13e-1 \pm 1e-4
FA_torch	6.88e-3 \pm 3.6e-5	3.3e-2 \pm 3.2e-5	1.29e-1 \pm 4.2e-5	5.14e-1 \pm 8.2e-5
LA	1.18e-4 \pm 1.3e-5	1.94e-4 \pm 4.8e-6	7.25e-4 \pm 1.7e-6	2.83e-3 \pm 7.4e-6
LA_torch	1e-3 \pm 9.7e-6	1.35e-3 \pm 8e-6	2.78e-3 \pm 3.2e-5	8.84e-3 \pm 5.2e-5
Recur	6.44e-4 \pm 7e-7	2.8e-3 \pm 5.7e-6	1.15e-2 \pm 1.5e-3	4.57e-2 \pm 6.1e-5

Method \ SeqLen	12,800	25,600	100,000
Vanilla	OOM	OOM	OOM
Bb	1.15e-1 \pm 1.8e-3	2.11e-1 \pm 1.9e-3	8.9e-1 \pm 2.4e-2
Cdotp	2.69e-2 \pm 5e-5	1.07e-1 \pm 7.6e-5	5.66e-1 \pm 7e-3
Cdotp_torch	1.39 \pm 5.5e-4	2.9 \pm 8.2e-2	1.11e1 \pm 8.9e-2
FA	1.77e-1 \pm 1.5e-4	3.58e-1 \pm 4.3e-4	1.41 \pm 1.7e-3
FA_torch	8.03e-1 \pm 6.7e-6	1.6 \pm 1.3e-5	6.25 \pm 1.7e-3
LA	4.45e-3 \pm 5.4e-6	8.69e-3 \pm 2e-5	4.31e-2 \pm 3.2e-3
LA_torch	1.35e-2 \pm 2.1e-4	2.65e-2 \pm 3.7e-4	9.96e-2 \pm 2.6e-4
Recur	9.12e-2 \pm 4.6e-5	1.82e-1 \pm 1.2e-4	7.35e-1 \pm 1e-3

5.1 Decoding extremely long prompts

We investigated the efficiency on a single-layer (exponentially decaying) causal linear attention module for the methods implemented in our library, across various prompt lengths⁴.

Inference latency was measured for prompt lengths ranging from 128 to 100,000 tokens. Table 3 and Table 4 show results with and without the exponentially decaying mask, both using a batch size of 1. Similarly, Table 6 and Table 5 show results with and without the exponentially decaying mask, both using a batch size of 16⁵.

Each measurement was replicated 15 times, and the final results are reported as the mean value and the standard deviation of each configuration.

Result analysis. As a sanity check, we could clearly observe that, as the sequence length of prompts increased, the latency of all the methods (except the **Vanilla** method) grew linearly. As shown in Table 3, when the batch size is 1, the **Vanilla** method incurs an OOM (out-of-memory) error once the sequence length surpasses 8,192, whereas other linear attention computation methods do not face this issue.

Additionally, Tables 3 and 4 indicate that, with a batch size of 1 and sequence length over 512, lightningAttention-2 (**LA**) is the fastest, outperforming other methods by at least a factor of two; while for short inputs (sequence length \leq 128), the **Vanilla** method, due to its simplistic design, is the best choice. In Table 4, it is also noted that the **Recur** method leads to an OOM error at a

⁴This experimentation was carried out on a 48GB NVIDIA A6000 GPU.

⁵Along all the tables in this paper, boldface represents the best result, and ‘‘OOM’’ denotes ‘‘out-of-memory’’.

Table 4: Measured latency (s) of single-layer attention with batch size 1 and exponentially decaying causal mask.

Method \ SeqLen	128	512	2,048	8,192
Vanilla	$1.12e-1 \pm 1.7e-3$	$5.08e-1 \pm 1.7e-3$	$2.593 \pm 8.2e-3$	$1.86e1 \pm 1.5e-1$
Bb	$5.53e-1 \pm 6.4e-2$	$3.25e-1 \pm 4.8e-2$	$5.4e-1 \pm 5.1e-2$	$5.56e-1 \pm 2.8e-2$
Cdotp	$2.36e-4 \pm 1.3e-7$	$9.28e-4 \pm 2.9e-6$	$3.68e-3 \pm 7.5e-6$	$1.66e-2 \pm 2.3e-5$
Cdotp_torch	$1.59e-2 \pm 3.2e-5$	$8.37e-2 \pm 5.5e-5$	$2.51e-1 \pm 5.7e-5$	$1.36 \pm 4.2e-4$
FA	$1.26e-3 \pm 8.2e-6$	$5.49e-3 \pm 2.7e-5$	$2.71e-2 \pm 1.4e-5$	$1.14e-1 \pm 1.2e-4$
FA_torch	$1.58e-2 \pm 7.3e-6$	$5.57e-2 \pm 1.8e-5$	$2.12e-1 \pm 3.5e-6$	$8.37e-1 \pm 1.4e-4$
LA	$1.27e-4 \pm 1.3e-5$	$1.96e-4 \pm 8e-7$	$7.49e-4 \pm 2.8e-6$	$2.9e-3 \pm 1.2e-5$
LA_torch	$1.21e-3 \pm 6.5e-6$	$1.56e-3 \pm 5e-6$	$3.45e-3 \pm 8.6e-5$	$1.18e-2 \pm 4.2e-4$
Recur	$2e-1 \pm 2.6e-3$	$8.1e-1 \pm 6.4e-3$	$3.17 \pm 2e-2$	$1.18e1 \pm 9.7e-2$

Method \ SeqLen	12,800	25,600	100,000
Vanilla	OOM	OOM	OOM
Bb	$8.53e-1 \pm 3.3e-2$	$9.26e-1 \pm 4.2e-2$	$1.69 \pm 3.7e-2$
Cdotp	$2.7e-2 \pm 7.7e-5$	$1.06e-1 \pm 6e-5$	$5.64e-1 \pm 7.4e-3$
Cdotp_torch	$1.54 \pm 8.6e-4$	$3.46 \pm 1.2e-1$	$1.26e1 \pm 1.6e-1$
FA	$1.78e-1 \pm 2e-4$	$3.59e-1 \pm 5.5e-4$	$1.42 \pm 1.9e-3$
FA_torch	$1.3 \pm 2.1e-5$	$2.6 \pm 3.5e-5$	$1.01e1 \pm 1.7e-4$
LA	$4.51e-3 \pm 1.4e-5$	$9.08e-3 \pm 1.5e-5$	$4.14e-2 \pm 2e-3$
LA_torch	$4.66e-3 \pm 2.5e-6$	$3.21e-2 \pm 4.1e-4$	$1.54e-1 \pm 3.7e-3$
Recur	$2.0e1 \pm 8.6e-3$	$3.41e2 \pm 1.5e2$	OOM

Table 5: Measured latency (s) of single-layer attention with batch size 16 without exponentially decaying causal mask.

Method \ SeqLen	128	512	2,048	8,192
Vanilla	$5.46e-4 \pm 3.4e-7$	$5.33e-3 \pm 1.2e-5$	$9.65e-2 \pm 2e-4$	OOM
Bb	$2.54e-3 \pm 1e-4$	$9.33e-3 \pm 1.1e-4$	$3.68e-2 \pm 8.6e-5$	$1.46e-1 \pm 4.6e-5$
Cdotp	$4.42e-4 \pm 1.5e-7$	$1.82e-3 \pm 7.9e-6$	$7.5e-3 \pm 2.4e-5$	$3.15e-2 \pm 6.6e-5$
Cdotp_torch	$3.31e-2 \pm 2.9e-6$	$1.32e-1 \pm 1.6e-5$	$5.31e-1 \pm 4.5e-5$	$2.12 \pm 1e-4$
FA	$1.85e-2 \pm 4.9e-5$	$7.42e-2 \pm 1.5e-4$	$3.92e-1 \pm 1.4e-3$	$1.48 \pm 1.8e-3$
FA_torch	$5.9e-2 \pm 5.8e-6$	$2.31e-1 \pm 3.7e-6$	$9.19e-1 \pm 8.2e-6$	$3.67 \pm 3.2e-5$
LA	$5.72e-4 \pm 6.6e-7$	$2.33e-3 \pm 8.6e-6$	$9.73e-3 \pm 3.4e-5$	$4e-2 \pm 1.2e-4$
LA_torch	$1.18e-2 \pm 2.3e-4$	$1.82e-2 \pm 3.2e-5$	$3.9 - 2 \pm 4.3e-5$	$1.18e-1 \pm 1.9e-4$
Recur	$1.49e-3 \pm 6.8e-5$	$8.6e-3 \pm 9.3e-5$	$4.36e-2 \pm 4.4e-5$	$2.12e-1 \pm 1e-4$

Method \ SeqLen	12,800	25,600	100,000
Vanilla	OOM	OOM	OOM
Bb	$2.31e-1 \pm 1e-4$	$4.65e-1 \pm 8.9e-5$	OOM
Cdotp	$4.71e-2 \pm 2.1e-5$	$9.97e-2 \pm 3.1e-4$	OOM
Cdotp_torch	$3.38 \pm 2.1e-4$	$7.04 \pm 4.5e-4$	OOM
FA	$2.31 \pm 1.1e-3$	$4.63 \pm 1.6e-3$	OOM
FA_torch	$5.75 \pm 5.9e-5$	$1.17e1 \pm 3.4e-5$	OOM
LA	$6.07e-2 \pm 3.5e-5$	$1.27e-1 \pm 3.9e-4$	OOM
LA_torch	$1.78e-1 \pm 2.6e-4$	$3.47e-1 \pm 1e-4$	OOM
Recur	$3.81e-1 \pm 2.8e-4$	$8.2e-1 \pm 3.3e-4$	OOM

Table 6: Measured latency (s) of single-layer attention with batch size 16 and exponentially decaying causal mask.

Method \ SeqLen	128	512	2,048	8,192
Vanilla	$1.12e-1 \pm 8.9e-4$	$5.43e-1 \pm 1.7e-2$	$2.77 \pm 2.8e-2$	OOM
Bb	$4.52e-2 \pm 2e-3$	$6.29e-2 \pm 7.8e-3$	$8.55e-2 \pm 6.2e-4$	$2.93e-1 \pm 1.8e-2$
Cdotp	$4.88e-4 \pm 7.3e-7$	$2.03e-3 \pm 1.1e-5$	$8.36e-3 \pm 2.2e-5$	$3.5e-2 \pm 1.1e-4$
Cdotp_torch	$4.58e-2 \pm 4.8e-6$	$1.83e-1 \pm 2e-5$	$7.34e-1 \pm 5.7e-5$	$2.93 \pm 8.5e-5$
FA	$1.85e-2 \pm 4.3e-5$	$7.49e-2 \pm 8.6e-5$	$3.9e-1 \pm 1.1e-3$	$1.48 \pm 1.5e-3$
FA_torch	$1.12e-1 \pm 1.3e-6$	$4.36e-1 \pm 2.1e-6$	$1.74 \pm 2.7e-5$	$6.98 \pm 7.1e-5$
LA	$6.52e-4 \pm 1.5e-6$	$2.57e-3 \pm 6.7e-6$	$1.05e-2 \pm 2.2e-5$	$4.28e-2 \pm 8.6e-5$
LA_torch	$1.15e-2 \pm 2e-4$	$1.98e-2 \pm 2e-5$	$4.49e-2 \pm 6.6e-5$	$1.41e-1 \pm 2.9e-4$
Recur	$1.87e-1 \pm 2.1e-3$	$7.4e-1 \pm 7.7e-4$	$2.98 \pm 4.1e-4$	$1.2e1 \pm 6.7e-3$

Method \ SeqLen	12,800	25,600	100,000
Vanilla	OOM	OOM	OOM
Bb	$3.39e-1 \pm 7.2e-4$	$1.31 \pm 3.3e-2$	OOM
Cdotp	$5.25e-2 \pm 3.3e-5$	$1.12e-1 \pm 2.3e-4$	OOM
Cdotp_torch	$4.64 \pm 3.2e-5$	$9.59 \pm 4.8e-4$	OOM
FA	$2.32 \pm 1.2e-3$	$4.65 \pm 1.9e-3$	OOM
FA_torch	$1.09e1 \pm 2.2e-5$	$2.165e1 \pm 1.1e-4$	OOM
LA	$6.49e-2 \pm 2.7e-5$	$1.34e-1 \pm 2.4e-4$	OOM
LA_torch	$2.13e-1 \pm 4.2e-4$	$4.16e-1 \pm 9.3e-5$	OOM
Recur	$2.1e1 \pm 7.6e-2$	OOM	OOM

sequence length of 100,000, possibly due to the excessive depth of recursion exceeding the GPU memory limit.

As shown in Tables 5 and 6, we observe that when the batch size is 16, the **Cdotp** method outperforms all the other methods across various sequence lengths. This superior performance is likely attributed to the CUDA optimizations applied to the batch size dimension. Additionally, for a given sequence length, increasing the batch size from 1 to 16 does not result in a $16\times$ increase in computational time, as parallel processing occurs along the batch size dimension, thereby enhancing GPU utilization. Furthermore, we observe that the methods implemented with CUDA perform $2\times\sim 20\times$ speedup than those implemented with PyTorch.

Suboptimality of the recursive strategy. As analyzed in Section 3.3, we observe that when the sequence length is smaller and there is no exponentially decaying causal mask, the performance of **Recur** is comparable to the best performance; the time consumption of recursion increases linearly with the sequence length.

However, when an exponentially decaying causal mask is used, the performance of **Recur** is significantly worse than that of other methods. Such a discrepancy is related to the base method it employs (in the original implementation of **Recur**, when the recursive sequence length falls below 32, the base method is invoked). For the cases with the exponentially decaying mask, the computation is performed directly using formulas written in PyTorch, whereas, for the scenario without an exponentially decaying causal mask, the causal-dot-product method is utilized.

Table 7: The wall time inference performance of TransNormerLLM-7B uses different methods to go through the dataset when the batch size is 1 and 2. The “original” method denotes the original attention computation method implemented in TransNormerLLM-7B.

Method \ Batch size	1		2	
	Avg Time(s)	Std	Avg Time(s)	Std
Original	64.6	0.0031	64.6	0.0026
Bb	83.6	0.0077	73.8	0.08
Cdotp	67.3	0.047	58.9	0.015
Cdotp_torch	268.0	1.4	159.0	0.16
FA	91.0	0.0018	88.0	0.06
FA_torch	308.0	0.0047	244.0	0.0024
LA	65.4	0.017	66.1	0.0034
LA_torch	63.5	0.027	63.6	0.035
Vanilla	3688	330	OOM	-
Recur	2539	36	1402	53

5.2 Effectiveness on linear transformers

We evaluated all the methods in the library w.r.t. the improved capability of prompt processing in LLMs. Experiment settings and result analysis are listed as follows.

Large language models. Specifically, we chose two open-source linear transformer large language models, TransNormerLLM-7B, and toy-retnet-1.3B. The two models both support exponentially decaying causal masks. More details are provided in Appendix A.1.

Datasets and protocols. To prepare longer prompts, we extracted samples from the LongBench (Bai et al., 2023) datasets. Specifically, we set the maximum sequence length to 8k based on our GPU memory size; i.e., we truncated the prompts with more than 8k tokens and filtered out the prompts shorter than 6k.

In this experiment, we executed the attention computing in an LLM with various baseline methods under two typical inference settings: the batch size is 1 or 2. Each experimental trial was conducted seven times. To reduce the impact of loading phase time variations, we excluded the highest and lowest time measurements and calculated the average of the remaining values to derive the final results. More information is in Appendix A.1.

Result analysis. From Tables 7 and 8, we can see that these linear attention computation methods significantly reduce GPU memory usage. As a clear evidence, when the batch size is set to 2 on TransNormerLLM-7B, these methods will not result in OOM errors.

We can observe that when the batch size is 2, the latency of each method is mostly lower than that when the batch size is 1; this is because when the batch size is 2, only half of the forward propagation is required for all the samples. In almost all the settings, **LA_torch** significantly outperformed the default **Original** method, which indicates the overhead of its CUDA version **LA** is non-negligible in these practical settings. Notably, **Cdotp**, implemented with the native CUDA, performed the best on TransNormerLLM-7B when the batch size is not 1, aligning with the observation in Section 5.1.

Table 8: The inference wall time of toy-retnet-1.3B uses different methods to go through the dataset when the batch size is 1 and 2. The **Original** method denotes the original attention computation method implemented in toy-retnet-1.3B.

Method \ Batch size	1		2	
	Avg Time(s)	Std	Avg Time(s)	Std
Original	47.4	0.25	40.7	0.15
Bb	77.9	0.62	53.7	0.17
Cdotp	39.6	0.11	36.4	0.075
Cdotp_torch	299.0	1.1	179.0	0.76
FA	64.8	0.068	62.6	0.045
FA_torch	374.0	0.29	285.0	0.18
LA	38.0	0.12	34.0	0.12
LA_torch	37.5	0.081	30.6	0.14
Vanilla	951.0	5	475.0	4.2
Recur	895.0	1.4	503.0	1.1

6 Conclusions

In this paper, we develop a software tool, `LeetDecoding`, to efficiently compute exponentially decaying causal linear attention in a single module or an existing linear transformer. We collect a bundle of computation methods from different application fields, most of which were not originally devoted to the computation of causal linear attention. We carefully analyze the computational complexity of those algorithms, provide the proof thereof as a reference in this paper, and propose/implement a new method `FleetAttention` in this package. Furthermore, we make non-trivial efforts to implement some applicable methods in GPU programming languages such as Triton or CUDA for notably faster performance compared to their native PyTorch counterparts; the implementation itself requires deep understanding of GPU architecture, proficient management of parallelization, and usage of numerous intricate techniques, while in developing applications with `LeetDecoding` all of those details are hidden from users.

Our implementation in `LeetDecoding` is particularly useful when addressing long sequence inputs, which motivates advancements in linear attention and facilitates more efficient processing of long texts in various business fields. Under various practical scenarios, each method exhibits distinct advantages due to the differences in computational processes; a universal subroutine, that selects the (empirically) optimal approach based on the input provided, is integrated in `LeetDecoding` as well.

Finally, we wish that this work will inspire the appearance of other open-sourced linear transformers that provides efficient language model services for data science applications in business analytics that can benefit from large language models.

Acknowledgments

We appreciate the valuable advice from Yuzhen Mao, Binhang Yuan, Sitian Chen, Amelie Chi Zhou, Weijia Chen, and Yihu Xu.

References

- Yushi Bai, Xin Lv, Jiajie Zhang, Hongchang Lyu, Jiankai Tang, Zhidian Huang, Zhengxiao Du, Xiao Liu, Aohan Zeng, Lei Hou, Yuxiao Dong, Jie Tang, and Juanzi Li. Longbench: A bilingual, multitask benchmark for long context understanding. *arXiv preprint arXiv:2308.14508*, 2023.
- Pierre Brugiere and Gabriel Turinici. Transformer for times series: an application to the s&p500, 2024. URL <https://arxiv.org/abs/2403.02523>.
- Antônio Junior Alves Caiado and Michael Hahsler. Ai content self-detection for transformer-based large language models. *arXiv preprint arXiv:2312.17289*, 2023.
- Yifan Chen, Qi Zeng, Heng Ji, and Yun Yang. Skyformer: Remodel self-attention with gaussian kernel and nyström method. *Advances in Neural Information Processing Systems*, 2021.
- Yifan Chen, Qi Zeng, Dilek Hakkani-Tur, Di Jin, Heng Ji, and Yun Yang. Sketching as a tool for understanding and accelerating self-attention for long sequences. In Marine Carpuat, Marie-Catherine de Marneffe, and Ivan Vladimir Meza Ruiz (eds.), *Proceedings of the 2022 Conference of the North American Chapter of the Association for Computational Linguistics: Human Language Technologies*, pp. 5187–5199, Seattle, United States, July 2022. Association for Computational Linguistics.
- Krzysztof Choromanski, Valerii Likhoshesterov, David Dohan, Xingyou Song, Andreea Gane, Tamas Sarlos, Peter Hawkins, Jared Davis, Afroz Mohiuddin, Lukasz Kaiser, et al. Rethinking attention with performers. *arXiv preprint arXiv:2009.14794*, 2020.
- Tri Dao, Daniel Y. Fu, Stefano Ermon, Atri Rudra, and Christopher Ré. Flashattention: Fast and memory-efficient exact attention with io-awareness, 2022.
- Jacob Devlin, Ming-Wei Chang, Kenton Lee, and Kristina Toutanova. Bert: Pre-training of deep bidirectional transformers for language understanding. *arXiv preprint arXiv:1810.04805*, 2018.
- Kwasi Joseph Dzahini and Stefan M. Wild. A class of sparse Johnson–Lindenstrauss transforms and analysis of their extreme singular values. *SIAM Journal on Matrix Analysis and Applications*, 2024. URL <https://arxiv.org/abs/2212.14858>. To appear.
- Groq. Groq raises \$640m to meet soaring demand for fast ai inference, Aug 2024. URL https://groq.com/news_press/groq-raises-640m-to-meet-soaring-demand-for-fast-ai-inference/.
- Albert Gu and Tri Dao. Mamba: Linear-time sequence modeling with selective state spaces. *arXiv preprint arXiv:2312.00752*, 2023.
- Insu Han, Rajesh Jayaram, Amin Karbasi, Vahab Mirrokni, David P. Woodruff, and Amir Zandieh. Hyperattention: Long-context attention in near-linear time, 2023.
- William B. Johnson and Joram Lindenstrauss. Extensions of lipschitz mappings into hilbert space. *Contemporary mathematics*, 26:189–206, 1984.
- Qiudan Li, David Jingjun Xu, Haoda Qian, Linzi Wang, Minjie Yuan, and Daniel Dajun Zeng. A fusion pretrained approach for identifying the cause of sarcasm remarks. *INFORMS Journal on Computing*, 2024.

-
- Lucas Dax Lingle. Transformer-VQ: Linear-time transformers via vector quantization. In *The Twelfth International Conference on Learning Representations*, 2024. URL <https://openreview.net/forum?id=oDdzXQzP2F>.
- Yiping Lu, Zhuohan Li, Di He, Zhiqing Sun, Bin Dong, Tao Qin, Liwei Wang, and Tie-Yan Liu. Understanding and improving transformer from a multi-particle dynamic system point of view, 2019. URL <https://arxiv.org/abs/1906.02762>.
- OpenAI. Techniques for training large neural networks. <https://openai.com/research/techniques-for-training-large-neural-networks>, 2022.
- Bo Peng, Eric Alcaide, Quentin Anthony, Alon Albalak, Samuel Arcadinho, Stella Biderman, Huanqi Cao, Xin Cheng, Michael Chung, Leon Derczynski, Xingjian Du, Matteo Grella, Kranthi Gv, Xuzheng He, Haowen Hou, Przemyslaw Kazienko, Jan Kocon, Jiaming Kong, Bartłomiej Koptyra, Hayden Lau, Jiaju Lin, Krishna Sri Ipsit Mantri, Ferdinand Mom, Atsushi Saito, Guangyu Song, Xiangru Tang, Johan Wind, Stanisław Woźniak, Zhenyuan Zhang, Qinghua Zhou, Jian Zhu, and Rui-Jie Zhu. RWKV: Reinventing RNNs for the transformer era. In Houda Bouamor, Juan Pino, and Kalika Bali (eds.), *Findings of the Association for Computational Linguistics: EMNLP 2023*, pp. 14048–14077, Singapore, December 2023. Association for Computational Linguistics.
- Hao Peng, Nikolaos Pappas, Dani Yogatama, Roy Schwartz, Noah Smith, and Lingpeng Kong. Random feature attention. In *International Conference on Learning Representations*, 2021.
- Ofir Press, Noah Smith, and Mike Lewis. Train short, test long: Attention with linear biases enables input length extrapolation. In *International Conference on Learning Representations*, 2022. URL <https://openreview.net/forum?id=R8sQPpGCv0>.
- Zhen Qin, Weixuan Sun, Hui Deng, Dongxu Li, Yunshen Wei, Baohong Lv, Junjie Yan, Lingpeng Kong, and Yiran Zhong. cosformer: Rethinking softmax in attention. In *International Conference on Learning Representations*, 2022. URL <https://openreview.net/forum?id=Bl8CQrx2Up4>.
- Zhen Qin, Dong Li, Weigao Sun, Weixuan Sun, Xuyang Shen, Xiaodong Han, Yunshen Wei, Baohong Lv, Xiao Luo, Yu Qiao, and Yiran Zhong. Transnormerllm: A faster and better large language model with improved transnormer, 2023.
- Zhen Qin, Weigao Sun, Dong Li, Xuyang Shen, Weixuan Sun, and Yiran Zhong. Lightning attention-2: A free lunch for handling unlimited sequence lengths in large language models, 2024.
- Ali Rahimi and Benjamin Recht. Random features for large-scale kernel machines. *Advances in neural information processing systems*, 20, 2007.
- Rwkv. Rwkv.cpp - is now being deployed to half a billion systems worldwidemaking it one of the world’s most widely deployed, truly open-source (apache2) ai solutions out thereas it now ships with every windows 11 system pic.twitter.com/u9g0sbes7u, Sep 2024. URL https://twitter.com/RWKV_AI/status/1831000938120917336.
- Yutao Sun, Li Dong, Shaohan Huang, Shuming Ma, Yuqing Xia, Jilong Xue, Jianyong Wang, and Furu Wei. Retentive network: A successor to transformer for large language models. *arXiv preprint arXiv:2307.08621*, 2023.
- Hu Tian, Xiaolong Zheng, Kang Zhao, Maggie Wenjing Liu, and Daniel Dajun Zeng. Inductive representation learning on dynamic stock co-movement graphs for stock predictions. *INFORMS journal on computing*, 34(4):1940–1957, 2022.

-
- Ashish Vaswani, Noam Shazeer, Niki Parmar, Jakob Uszkoreit, Llion Jones, Aidan N Gomez, Łukasz Kaiser, and Illia Polosukhin. Attention is all you need. *Advances in neural information processing systems*, 30, 2017.
- Apoorv Vyas, Angelos Katharopoulos, and François Fleuret. Fast transformers with clustered attention. *Advances in Neural Information Processing Systems*, 33:21665–21674, 2020.
- Sinong Wang, Belinda Z. Li, Madian Khabsa, Han Fang, and Hao Ma. Linformer: Self-attention with linear complexity, 2020.
- Yongtao Wu, Fanghui Liu, Grigorios Chrysos, and Volkan Cevher. On the convergence of encoder-only shallow transformers. In *Thirty-seventh Conference on Neural Information Processing Systems*, 2023. URL <https://openreview.net/forum?id=8ZveVHfmIE>.
- Songlin Yang, Bailin Wang, Yikang Shen, Rameswar Panda, and Yoon Kim. Gated linear attention transformers with hardware-efficient training, 2023.
- Tiankai Yang, Yi Nian, Shawn Li, Ruiyao Xu, Yuangang Li, Jiaqi Li, Zhuo Xiao, Xiyang Hu, Ryan Rossi, Kaize Ding, Xia Hu, and Yue Zhao. Ad-llm: Benchmarking large language models for anomaly detection, 2024. URL <https://arxiv.org/abs/2412.11142>.
- Yi Yang, Kunpeng Zhang, and Yangyang Fan. Analyzing firm reports for volatility prediction: A knowledge-driven text-embedding approach. *INFORMS Journal on Computing*, 34(1):522–540, 2022.
- Lin Zheng, Chong Wang, and Lingpeng Kong. Linear complexity randomized self-attention mechanism. In *International Conference on Machine Learning*, pp. 27011–27041. PMLR, 2022.

Appendices to “LeetDecoding: A PyTorch Library for Exponentially Decaying Causal Linear Attention with CUDA Implementations”

A More on Experiments

A.1 Evaluation on linear transformers

In Section 5.2, we used TransNormerLLM-7B and toy-retnet-1.3B as the base model to test the implemented methods, on a dataset adapted from the LongBench dataset.

Since the NVIDIA A6000 GPU used in our experiment solely has 48G memory, the model cannot handle particularly long prompts. In order to allow the model to handle longer prompts, ❶ we retained the first two layers of the models for inference, so that more memory in the GPU could be used for calculations rather than storage of model weight parameters. ❷ Moreover, we truncated the prompts in LongBench to 8k tokens using the tokenizer of TransNormerLLM-7B. At the same time, we removed questions with length less than 6k. Consequently, we get an crafted evaluation dataset with 100 prompt samples.

In addition, as toy-retnet-1.3B only supports the fp32 data type, fp32 numerical precision is adopted along the experiments. To alleviate the impacts of the GPU startup time in benchmarking computation methods, we conducted 7 experiments in succession; we next removed the maximum and minimum results, and then computed the reported statistics on the remaining results, such as the average value and the sample standard deviation.

A.2 License information

TransNormerLLM-7B model is licensed under the Apache 2.0 License.

toy-retnet-1.3B model is licensed under the Apache 2.0 License.

LongBench is licensed under the MIT License.

B Algorithm Details

B.1 The “row-based” algorithm behind `causal-dot-product_torch`

Choromanski et al. (2020, Equation (11)) introduced a prefix sum algorithm for causal linear attention. In each iteration, it returns one row of the output matrix, and we thus refer to this algorithm as the “row-based algorithm.”

Vectors $\mathbf{c}_j, \mathbf{b}_j \in \mathbb{R}^{1 \times r}$, and $\mathbf{v}_j \in \mathbb{R}^{1 \times d}$ represent the j -th row-vectors in matrices $\mathbf{C}, \mathbf{B}, \mathbf{V}$, respectively. A single row of the output matrix \mathbf{O} is then computed as:

$$\mathbf{O}_i = \sum_{j=1}^i \mathbf{b}_i \mathbf{c}_j^T \mathbf{v}_j = \mathbf{b}_i \sum_{j=1}^i \mathbf{c}_j^T \mathbf{v}_j \in \mathbb{R}^{1 \times d} \quad (7)$$

Let $\mathbf{U}_i = \sum_{j=1}^i \mathbf{c}_j^T \mathbf{v}_j \in \mathbb{R}^{r \times d}$, then Equation (7) can be realized through recursion:

$$\mathbf{O}_i = \mathbf{b}_i \mathbf{U}_i, \quad \text{where } \mathbf{U}_i = \mathbf{U}_{i-1} + \mathbf{c}_i^T \mathbf{v}_i. \quad (8)$$

The full row-based algorithm is described in Algorithm 1. The time complexity for processing each row of \mathbf{O} is $\mathcal{O}(rd)$, leading to a total time complexity of $\mathcal{O}(Nrd)$. The space complexity is $\mathcal{O}(Nd + rd)$.

Algorithm 1 Row-based Algorithm

Require: Matrices $\mathbf{B}, \mathbf{C} \in \mathbb{R}^{N \times r}$, $\mathbf{V} \in \mathbb{R}^{N \times d}$.

- 1: Initialize $\mathbf{U} = (\mathbf{0})_{r \times d} \in \mathbb{R}^{r \times d}$, $\mathbf{O} = (\mathbf{0})_{N \times d} \in \mathbb{R}^{N \times d}$.
 - 2: **for** $1 \leq i \leq N$ **do**
 - 3: Extract row vectors $\mathbf{b}_i \in \mathbb{R}^{1 \times r}$, $\mathbf{c}_i \in \mathbb{R}^{1 \times r}$, $\mathbf{v}_i \in \mathbb{R}^{1 \times d}$ from $\mathbf{B}, \mathbf{C}, \mathbf{V}$ respectively.
 - 4: Update $\mathbf{U} \leftarrow \mathbf{U} + \mathbf{c}_i^T \mathbf{v}_i$.
 - 5: Compute $\mathbf{o}_i = \mathbf{b}_i \mathbf{U}$.
 - 6: Store $\mathbf{O}_i = \mathbf{o}_i$.
 - 7: **end for**
 - 8: Return the output \mathbf{O} .
-

B.2 Block-based Algorithm

The row-by-row computation algorithm described in Equation (8) is considered to be inefficient. Transformer-VQ (Lingle, 2024, Equation (28)) proposed a block-by-block computation method designed for its specific low-rank matrix operations. We extend this method to a general low-rank matrix product $\tilde{\mathbf{A}} = \mathbf{BC}$.

Let the block size be denoted as B_c . The block slice $[iB_c : (i+1)B_c]$ is abbreviated as $[i]$. Let $\hat{\mathbf{K}} \in \mathbb{R}^{N \times k}$ be the approximation of \mathbf{K} obtained through the low-rank method in Transformer-VQ or other algorithms. Let $\mathbf{M} \in \{0, 1\}^{B_c \times B_c}$ be a lower triangular causal mask, where $\mathbf{M}_{ij} = 1$ if $j \leq i$ and $\mathbf{M}_{ij} = 0$ otherwise. Then the general computation method can present as follows:

$$\mathbf{O}_{[i]} = (\exp(\mathbf{Q}_{[i]} \hat{\mathbf{K}}_{[i]}^T) \odot \mathbf{M}) \mathbf{V}_{[i]} + \sum_{j=1}^i \exp(\mathbf{Q}_{[i]} \hat{\mathbf{K}}_{[j]}^T) \mathbf{V}_j \quad (9)$$

$$= (\mathbf{B}_{[i]} \mathbf{C}_{[i]}^T \odot \mathbf{M}) \mathbf{V}_{[i]} + \sum_{j=1}^i \mathbf{B}_{[i]} \mathbf{C}_{[j]}^T \mathbf{V}_j \quad (10)$$

$$= (\mathbf{B}_{[i]} \mathbf{C}_{[i]}^T \odot \mathbf{M}) \mathbf{V}_{[i]} + \mathbf{B}_{[i]} \sum_{j=1}^i \mathbf{C}_{[j]}^T \mathbf{V}_j \quad (11)$$

Let $\mathbf{U}_{[i]} = \sum_{j=1}^i \mathbf{C}_{[j]}^T \mathbf{V}_{[j]} \in \mathbb{R}^{d \times d}$. Then, we obtain:

$$\mathbf{O}_{[i]} = (\mathbf{B}_{[i]} \mathbf{C}_{[i]}^T \odot \mathbf{M}) \mathbf{V}_{[i]} + \mathbf{B}_{[i]} \mathbf{U}_{[i-1]} \quad (12)$$

$$\mathbf{U}_{[i]} = \mathbf{U}_{[i-1]} + \mathbf{C}_{[i]}^T \mathbf{V}_{[i]} \quad (13)$$

The full block-based algorithm is described in Algorithm 2. The time complexity for processing each block $\mathbf{O}_{[i]}$ is $\mathcal{O}(B_c^2 r + B_c^2 d + B_c r d)$; there are $\lceil \frac{N}{B_c} \rceil$ blocks, leading to a total time complexity of $\mathcal{O}(NB_c r + NB_c d + Nrd)$. If we set $B_c = \mathcal{O}(d)$, the time and space complexity are $\mathcal{O}(Nrd)$ and $\mathcal{O}(Nd + rd)$, respectively.

B.3 Recursion Algorithm

HyperAttention (Han et al., 2023, Algorithm (4)) proposes a recursive method to compute causal attention. This approach starts with partitioning the matrices into two distinct parts: one is masked and the other remains unmasked. Following this initial division, the method further recursively partitions the masked part while concurrently applying computation method to the unmasked areas.

Algorithm 2 block-based Algorithm

Require: Matrices $\mathbf{B}, \mathbf{C} \in \mathbb{R}^{N \times r}$, $\mathbf{V} \in \mathbb{R}^{N \times d}$, block size B_c .

- 1: Divide \mathbf{V} into $T_c = \lceil \frac{N}{B_c} \rceil$ blocks $\mathbf{V}_{[1]}, \dots, \mathbf{V}_{[T_c]}$ of size $B_c \times d$ each.
 - 2: Divide \mathbf{B}, \mathbf{C} into T_c blocks $\mathbf{B}_{[1]}, \dots, \mathbf{B}_{[T_c]}; \mathbf{C}_{[1]}, \dots, \mathbf{C}_{[T_c]}$; of size $B_c \times r$ each.
 - 3: Initialize $\mathbf{U} = (\mathbf{0})_{r \times d} \in \mathbb{R}^{r \times d}$, $\mathbf{O} = (\mathbf{0})_{N \times d} \in \mathbb{R}^{N \times d}$.
 - 4: Let $\mathbf{M} \in \{0, 1\}^{B_c \times B_c}$ be a lower triangular causal mask.
 - 5: **for** $0 \leq i < T_c$ **do**
 - 6: Compute $\mathbf{o} = (\mathbf{B}_{[i]} \mathbf{C}_{[i]}^T \odot \mathbf{M}) \mathbf{V}_{[i]} + \mathbf{B}_{[i]} \mathbf{U}$.
 - 7: Update $\mathbf{U} \leftarrow \mathbf{U} + \mathbf{C}_{[i]}^T \mathbf{V}_{[i]}$.
 - 8: Compute and store $\mathbf{O}_{[i]} = \mathbf{o}$.
 - 9: **end for**
 - 10: Return the output \mathbf{O} .
-

Algorithm 3 recursion Algorithm

Require: Matrices $\mathbf{B}, \mathbf{C}, \mathbf{V}$.

- 1: **if** $\text{len}(\mathbf{B}) \leq \text{termination block size}$ **then**
 - 2: Return $(\mathbf{M} \odot \mathbf{B} \mathbf{C}^T) \mathbf{V}$
 - 3: **else**
 - 4: Split $\mathbf{B}, \mathbf{C}, \mathbf{V}$ into equal sized sub-matrices: $\mathbf{B}_1, \mathbf{B}_2; \mathbf{C}_1, \mathbf{C}_2; \mathbf{V}_1, \mathbf{V}_2$.
 - 5: $\mathbf{O}_1 \leftarrow \text{Recursion}(\mathbf{B}_1, \mathbf{C}_1, \mathbf{V}_1)$
 - 6: $\mathbf{O}_2 \leftarrow \text{Recursion}(\mathbf{B}_2, \mathbf{C}_2, \mathbf{V}_2)$
 - 7: $\mathbf{O}_3 \leftarrow \mathbf{B}_2 (\mathbf{C}_1^T \mathbf{V}_1)$
 - 8: Return $\begin{bmatrix} \mathbf{O}_1 & \mathbf{0} \\ \mathbf{O}_3 & \mathbf{O}_2 \end{bmatrix}$
 - 9: **end if**
-

We have extended the recursive approach to the general low-rank matrix form in Equation (4). We divide $\mathbf{B}, \mathbf{C}, \mathbf{V}$ recursively to enable more efficient computation of the causal attention. As shown in Figure 1, the masked attention matrix $\tilde{\mathbf{A}} \odot \mathbf{M}$ can be decomposed into three distinct non-zero submatrices, each half the size of the original attention matrix. Notably, the block $\mathbf{B}_{(2)} \mathbf{C}_{(1)}$, located entirely below the diagonal is unmasked attention. We can efficiently compute this part of the result as $\mathbf{B}_{(2)} (\mathbf{C}_{(1)} \mathbf{V}_{(1)})$, enabling linear computation through right multiplication. The two diagonal blocks $\mathbf{B}_{(1)} \mathbf{C}_{(1)} \odot \mathbf{M}$ and $\mathbf{B}_{(2)} \mathbf{C}_{(2)} \odot \mathbf{M}$ in Fig. 1 represent causal attentions with half the original size. To compute these, we recursively partition them into even smaller blocks and repeat such a decomposition procedure. The full recursion algorithm is described in Algorithm 3 and Algorithm 4.

B.4 FleetAttention: An IO-aware Implementation

The ideal implementation of FleetAttention on GPU is non-trivial. With vanilla Einstein sum operations, we will need $\mathcal{O}(Ndr)$ space to store r summands for the final sum up. It is thus necessary to balance the GPU memory usage and the computation speed, as in regular matrix multiplication on GPU. To address this, we introduce an IO-aware implementation, which maintains the computational complexity at $\mathcal{O}(Ndr)$ while reducing the space complexity to $\mathcal{O}(Nd)$.

FleetAttention leverages the tiling technique (Dao et al., 2022) to enhance memory access efficiency between the GPU High Bandwidth Memory (HBM) and its on-chip Static Random-Access Mem-

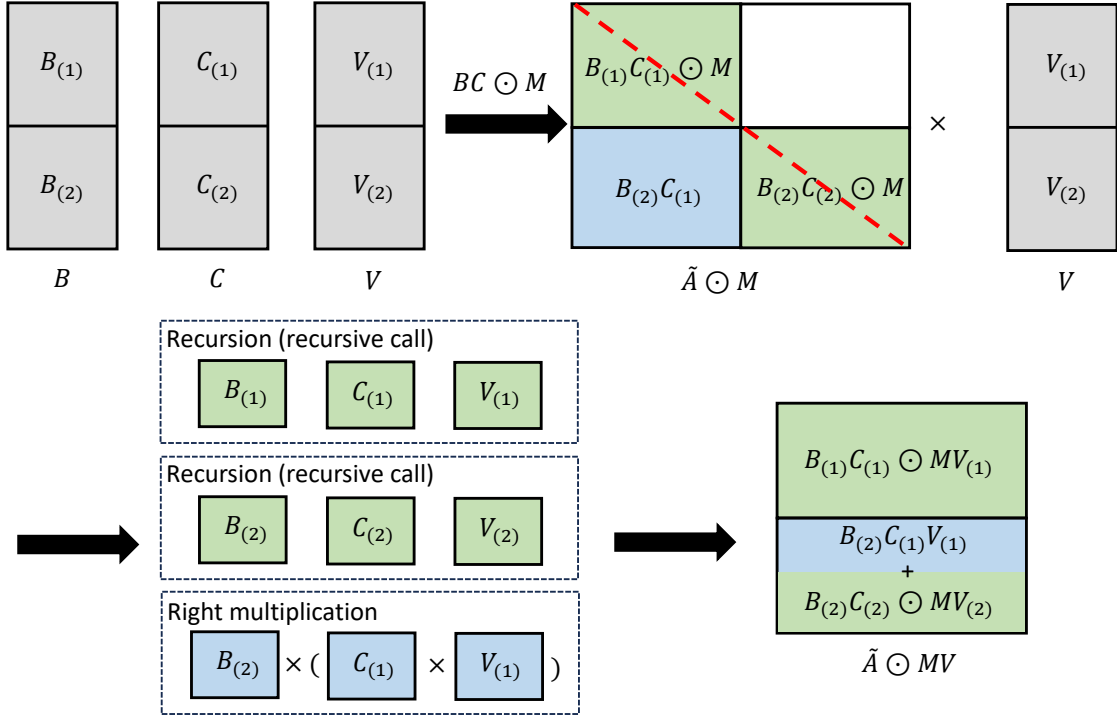


Figure 1: Visualization of the Recursion algorithm. Causal attention matrix can be divided into three equal-sized non-zero sections: $B_{(1)}C_{(1)} \odot M$ and $B_{(2)}C_{(2)} \odot M$ are both masked attention score matrices and $B_{(2)}C_{(1)}$ is an unmasked attention score matrix.

Algorithm 4 recursion Algorithm with special mask

Require: Matrices B, C, V, w , left, right.

- 1: **if** $\text{len}(B) \leq \text{termination block size}$ **then**
 - 2: $M_s = \text{GetMask}(\text{right-left}, w)$
 - 3: **Return** $(M_s \odot BC^T)V$
 - 4: **else**
 - 5: Split B, C, V into equal sized sub-matrices: $B_1, B_2; C_1, C_2; V_1, V_2$. $\text{mid} = \lfloor \frac{\text{left+right}}{2} \rfloor$
 - 6: $O_1 \leftarrow \text{Recursion}(B_1, C_1, V_1, w, \text{left}, \text{mid})$
 - 7: $O_2 \leftarrow \text{Recursion}(B_2, C_2, V_2, w, \text{mid}, \text{right})$
 - 8: $W_1 = [1, w, w^2, \dots, w^{\text{right-mid-1}}]$, $W_2 = [w^{\text{mid-left}}, w^{\text{mid-left-1}}, \dots, w]$
 - 9: $O_3 \leftarrow (\text{diag}(W_1)B_2)((\text{diag}(W_2)C_1)^T V_1)$
 - 10: **Return** $\begin{bmatrix} O_1 & \mathbf{0} \\ O_3 & O_2 \end{bmatrix}$
 - 11: **end if**
-

ory (SRAM). Meanwhile, this method mitigates memory overflow when dealing with long sequence lengths. The time and memory efficiency of this method are reported in Section 5.1.

The core idea of our optimization is that we split the input matrices B, C, V into blocks. These blocks are then loaded from the slow HBM into the fast SRAM, where the attention outputs are computed w.r.t. these blocks. We simultaneously apply the appropriate normalization factors to the outputs of each block, ensuring the accuracy of the results. Specifically, since the computation for

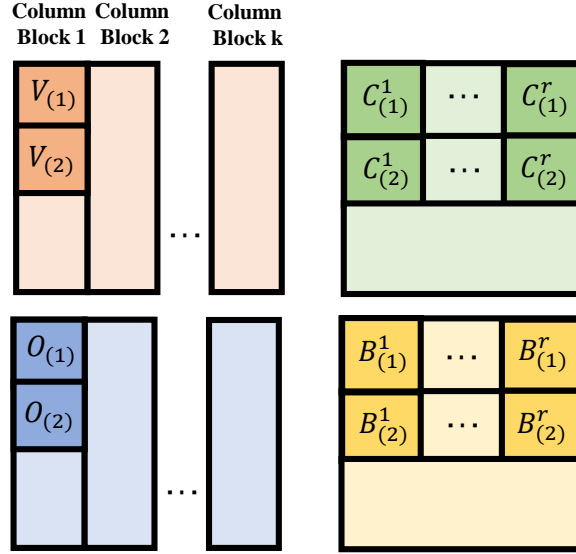


Figure 2: Matrices splitting in FleetAttention

each column of \mathbf{V} in Equation (5) is independent, we can split \mathbf{V} into column blocks for parallel computation. Moreover, an entire column block may still exceed the SRAM memory, we further subdivide each column block into row blocks, as illustrated in Figure 2. This ensures that the sub-matrices can fit entirely into SRAM, allowing us to complete all operations for a given sub-matrix consecutively.

The computation process is described below. To simplify, we focus on a single column block of the value matrix \mathbf{V} , divided into $\begin{bmatrix} \mathbf{V}_{(1)} \\ \mathbf{V}_{(2)} \end{bmatrix}$ for some matrices $\mathbf{V}_{(1)}, \mathbf{V}_{(2)} \in \mathbb{R}^{B_r \times B_c}$, where B_r and B_c are the row and column block sizes, respectively. Our objective is to calculate the attention output \mathbf{O} for this column block, which takes a similar form $\begin{bmatrix} \mathbf{O}_{(1)} \\ \mathbf{O}_{(2)} \end{bmatrix}$ for some metrics $\mathbf{O}_{(1)}, \mathbf{O}_{(2)} \in \mathbb{R}^{B_r \times B_c}$. We have two matrices \mathbf{B} and \mathbf{C} , of the low-rank approximation form

$$\mathbf{C} = \begin{bmatrix} \mathbf{C}_{(1)}^1, \dots, \mathbf{C}_{(1)}^r \\ \mathbf{C}_{(2)}^1, \dots, \mathbf{C}_{(2)}^r \end{bmatrix}, \quad \mathbf{B} = \begin{bmatrix} \mathbf{B}_{(1)}^1, \dots, \mathbf{B}_{(1)}^r \\ \mathbf{B}_{(2)}^1, \dots, \mathbf{B}_{(2)}^r \end{bmatrix},$$

where $\mathbf{B}_{(1)}^i, \mathbf{B}_{(2)}^i, \mathbf{C}_{(1)}^i, \mathbf{C}_{(2)}^i \in \mathbb{R}^{B_r \times 1}$ are columns of matrices.

For the first block $\mathbf{V}_{(1)}$, according to Equation (5), we can obtain

$$\mathbf{O}_{(1)} = \sum_{i=1}^r \text{diag}(\mathbf{B}_{(1)}^i) \text{cumsum}(\text{diag}(\mathbf{C}_{(1)}^i) \mathbf{V}_{(1)}),$$

where $\text{cumsum}(\cdot)$ returns a matrix of the same shape as the input, representing the cumulative sum of elements along the matrix's vertical direction. To facilitate the cumsum operation in the subsequent block, we cached the prefix sums of this block:

$$\mathbf{l}_{(1)}^i = \text{sum}(\text{diag}(\mathbf{C}_{(1)}^i) \mathbf{V}_{(1)})$$

where $\text{sum}(\cdot)$ returns a row vector that is the sum of all the rows in the matrix. For subsequent blocks, we add prefix sums at the corresponding positions to ensure the accuracy of the results and

Algorithm 5 FleetAttention

Require: Matrices $\mathbf{B}, \mathbf{C} \in \mathbb{R}^{N \times r}$, $\mathbf{V} \in \mathbb{R}^{N \times d}$ in HBM, block sizes B_c, B_r .

- 1: Divide \mathbf{V} into $T_c = \lceil \frac{d}{B_c} \rceil$ blocks $\mathbf{V}^1, \dots, \mathbf{V}^{T_c}$ of size $N \times B_c$ each, then devide \mathbf{V}^k into $T_r = \lceil \frac{N}{B_r} \rceil$ blocks $\mathbf{V}_1^k, \dots, \mathbf{V}_{T_r}^k$ of size $B_r \times B_c$ each.
 - 2: Divide \mathbf{B} into $T_r \times r$ column blocks $\mathbf{B}_1^1, \dots, \mathbf{B}_1^r, \dots, \mathbf{B}_{T_c}^1, \dots, \mathbf{B}_{T_c}^r$ of size $B_r \times 1$ each.
 - 3: Divide \mathbf{C} into $T_r \times r$ column blocks $\mathbf{C}_1^1, \dots, \mathbf{C}_1^r, \dots, \mathbf{C}_{T_c}^1, \dots, \mathbf{C}_{T_c}^r$ of size $B_r \times 1$ each.
 - 4: Divide the output \mathbf{O} into T_c blocks $\mathbf{O}^1, \dots, \mathbf{O}^{T_c}$ of size $N \times B_c$ each, then devide \mathbf{O}^k into T_r blocks $\mathbf{O}_1^k, \dots, \mathbf{O}_{T_r}^k$ of size $B_r \times B_c$ each.
 - 5: **for** $1 \leq k \leq T_c$, parallel computation of \mathbf{O}^k **do**
 - 6: $\mathbf{l}^0, \dots, \mathbf{l}^r = (\mathbf{0})_{B_c} \in \mathbb{R}^{B_c}$
 - 7: **for** $1 \leq i \leq T_r$ **do**
 - 8: Load \mathbf{V}_i^k from HBM to on-chip SRAM.
 - 9: On chip, initialize $\mathbf{O}_i^k = (\mathbf{0})_{B_r \times B_c} \in \mathbb{R}^{B_r \times B_c}$.
 - 10: **for** $1 \leq j \leq r$ **do**
 - 11: Load $\mathbf{B}_i^j, \mathbf{C}_i^j$ from HBM to on-chip SRAM.
 - 12: On chip, compute $\mathbf{O}_i^k \leftarrow \mathbf{O}_i^k + \text{diag}(\mathbf{B}_i^j)(\text{cumsum}(\text{diag}(\mathbf{C}_i^j)\mathbf{V}_i^k) + \mathbf{l}^j)$.
 - 13: On chip, compute $\mathbf{l}^j \leftarrow \text{sum}(\text{diag}(\mathbf{C}_i^j)\mathbf{V}_i^k) + \mathbf{l}^j$
 - 14: **end for**
 - 15: Write \mathbf{O}_i^k to HBM as the block of \mathbf{O}_i^k .
 - 16: **end for**
 - 17: **end for**
 - 18: Return the output \mathbf{O} .
-

continue updating the prefix sums. The following recursive formula can be derived:

$$\begin{aligned}\mathbf{O}_{(n)} &= \sum_{i=1}^r \text{diag}(\mathbf{B}_{(n)}^i)(\text{cumsum}(\text{diag}(\mathbf{C}_{(n)}^i)\mathbf{V}_{(n)}) + \mathbf{l}_{(n-1)}^i) \\ \mathbf{l}_{(n)}^i &= \text{sum}(\text{diag}(\mathbf{C}_{(n)}^i)\mathbf{V}_{(n)}) + \mathbf{l}_{(n-1)}^i\end{aligned}$$

The full procedure of FleetAttention is given in Algorithm 5, and we implemented it in Triton in LeetDecoding.

B.5 Details about CUDA Implementations

causal-dot-product natively supported only the 32-bit floating-point (fp32) type and the classic causal linear attention calculations with masks consisting exclusively of 0s and 1s. We have extended this by implementing a half-precision (16-bit floating-point) version using CUDA, enabling its application in popular linear transformer large language models. Additionally, the method now supports exponentially decaying masks, further enhancing its versatility and performance.

lightningAttention-2 is written in OpenAI’s Triton programming language, and the official implementation of **lightningAttention-2** natively supports only 16-bit floating-point computations and is deeply tied to specific GPU; i.e., it could only run on GPUs such as Nvidia A100 or more advanced, otherwise users will encounter resource limitations. We thoroughly optimized the implementation to support 32-bit floating-point computations and adjusted parameters for different GPUs, enabling its use for GPUs less advanced than A100.

Our proposed **FleetAttention** has two implementations: PyTorch and Triton. The PyTorch version is simple to use, and the algorithm is described in Equation (5). The Triton version is much more complicated, mainly because it needs to consider parallelization to maximize the utilization of GPU cores. In addition, since the GPU memory is limited, in the implementation we specifically tweak how to set the scale of parallel operations.

C Derivations Omitted in the Main Text

C.1 Generalization of FleetAttention to Attention with Exponentially Decaying Positional Embedding

In the specific attention variant with exponentially decaying positional embedding, we have a slightly different mask matrix

$$\mathbf{M} = [\lambda^{i-j} \cdot \delta(i, j)], \quad \text{with the discount factor } \lambda \in (0, 1],$$

which is still a lower triangular matrix. With the notation above, the original causal attention matrix can be taken as a special case with $\lambda = 1$.

We first study a toy case, in which the i -th row of the product $\mathbf{O} = \mathbf{M}\mathbf{V}$ (i.e., \mathbf{B}, \mathbf{C} is an all-one column vector), and have

$$\begin{aligned} \mathbf{O}_{i,:} &= \sum_{j=1}^i \lambda^{i-j} \mathbf{V}_{j,:} = \mathbf{V}_{i,:} + \sum_{j=1}^{i-1} \lambda^{i-j} \mathbf{V}_{j,:} = \mathbf{V}_{i,:} + \lambda \left(\sum_{j=1}^{i-1} \lambda^{i-1-j} \mathbf{V}_{j,:} \right) \\ &= \mathbf{V}_{i,:} + \lambda \mathbf{O}_{i-1,:}. \end{aligned}$$

We note the operator \mathbf{M} is now equivalent to the so-called discounted cumsum operator, which enjoys the linear $\mathcal{O}(N)$ complexity as well.

Denoting the discounted cumsum operator as λ -cumsum, we combine the pieces above and have

$$\begin{aligned} \mathbf{O} &= \left((\mathbf{B}\mathbf{C}^T) \odot \mathbf{M} \right) \mathbf{V} = \sum_{i=1}^r \text{diag}(\mathbf{b}_i) \mathbf{M} \text{diag}(\mathbf{c}_i) \mathbf{V} \\ &= \sum_{i=1}^r \text{diag}(\mathbf{b}_i) \cdot \lambda\text{-cumsum}(\text{diag}(\mathbf{c}_i) \mathbf{V}). \end{aligned}$$

Therefore, the complexity analysis of our algorithm in Section 3.1 still applies, and we conclude the generalized version of FleetAttention maintains $\mathcal{O}(N)$ time complexity.

C.2 Proof of Lemma 3.1

Proof. We first call $\mathbf{B}, \mathbf{C} \in \mathbb{R}^{N \times r}$, $\mathbf{V} \in \mathbb{R}^{N \times d}$ which satisfies $N \gg d$ and $N \gg r$. \mathbf{M} is a 0-1 matrix with elements in the lower triangle all one. $\tilde{\mathbf{A}}\mathbf{V} = \mathbf{B}\mathbf{C} \odot \mathbf{M}\mathbf{V}$ can be rewritten in a partitioned manner:

$$\begin{pmatrix} \mathbf{B}_1 \\ \mathbf{B}_2, \end{pmatrix} (\mathbf{C}_1, \mathbf{C}_2) \odot \mathbf{M} \begin{pmatrix} \mathbf{V}_1 \\ \mathbf{V}_2, \end{pmatrix} = \begin{pmatrix} \mathbf{B}_1 \mathbf{C}_1 \odot \mathbf{M}, \mathbf{0} \\ \mathbf{B}_2 \mathbf{C}_1, \mathbf{B}_2 \mathbf{C}_2 \odot \mathbf{M} \end{pmatrix} \begin{pmatrix} \mathbf{V}_1 \\ \mathbf{V}_2, \end{pmatrix} = \begin{pmatrix} \mathbf{B}_1 \mathbf{C}_1 \odot \mathbf{M}\mathbf{V}_1 \\ \mathbf{B}_2 \mathbf{C}_1 \mathbf{V}_1 + \mathbf{B}_2 \mathbf{C}_2 \odot \mathbf{M}\mathbf{V}_2 \end{pmatrix}$$

For the formula $\mathbf{B}_1 \mathbf{C}_1 \odot \mathbf{M}\mathbf{V}_1$ and $\mathbf{B}_2 \mathbf{C}_2 \odot \mathbf{M}\mathbf{V}_2$ we can use the method just now to further recurse. For the formula $\mathbf{B}_2 \mathbf{C}_1 \mathbf{V}_1$ we can use right multiplication which has a time complexity of $\mathcal{O}(N)$.

Table 9: Runtime analysis of the single-layer attention for both FleetAttention and FleetAttention_modify methods. The “bz” column represents the batch size. The “exp. decay” column indicates whether an exponentially decaying causal mask is used.

Method \ SeqLen	SeqLen	bz	exp. decay	128	512	2048	8192	12800	25600	100000
FA	1	1	✗	1.26e-3	5.46e-3	2.72e-2	1.13e-1	1.77e-1	3.58e-1	1.41
FA	1	1	✓	1.26e-3	5.49e-3	2.71e-2	1.14e-1	1.78e-1	3.59e-1	1.42
FA	16	16	✗	1.85e-2	7.42e-2	3.92e-1	1.48	2.31	4.63	OOM
FA	16	16	✓	1.85e-2	7.49e-2	3.90e-1	1.48	2.32	4.65	OOM
FA_modify	1	1	✗	7.00e-4	3.31e-3	1.32e-2	5.28e-2	8.27e-2	1.65e-1	6.55e-1
FA_modify	1	1	✓	7.17e-4	3.33e-3	1.33e-2	5.43e-2	8.34e-2	1.68e-1	6.65e-1
FA_modify	16	16	✗	1.18e-2	5.12e-2	2.06e-1	8.36e-1	1.31	2.60	OOM
FA_modify	16	16	✓	1.18e-2	5.15e-2	2.05e-1	8.14e-1	1.33	2.65	OOM

According to the above recursion relationship, we can get the time complexity expression:

$$\begin{aligned}
 T(N) &= 2T(N/2) + N \\
 \text{Master theorem : } T(N) &= aT(N/b) + f(N) \\
 \text{So : } a &= 2, b = 2, f(N) = N. \\
 f(N) &= \Theta(N^{\log_b a}) = \Theta(N) \\
 \text{then : } T(N) &= \Theta(N \lg N)
 \end{aligned}$$

The claim in Lemma 3.1 is then attained. ◇

D A finer performance analysis of FleetAttention

The FleetAttention (FA as a shorthand) method performs the sum operations across the rank dimension as an “atomic operation”. This “atomic operation” necessarily hinders the execution of the FA method, while we have to set it as atomic to prevent data inconsistency.

To explore the potential benefit of accelerating this “atomic operation”, we modified its Triton implementation (named FleetAttention_modify, or FA_modify in short) so that the sum operations across the rank dimension now occurs directly after loading the data, before writing it back. This modification means the operation is no longer atomic, potentially causing the situation where other parallel ranks may load the data (this modification can result in data inconsistency and thus not incorporated in LeetDecoding).

We have conducted a runtime analysis of both methods following the same experiment setup in Section 5.1. The results are summarized in Table 9. Under various conditions, where the batch size is either 1 or 16, and the sequence length ranges from 128 to 100,000, the FA_modify method consistently requires approximately half the time compared to the FA method. This indicates that parallelizing in the rank dimension indeed affects the performance of the algorithm at the point where results are accumulated.